4. EXPERIMENTAL VERIFICATION

As shown in Figure 6, a scanning acoustic microscopy (SAM) system was designed for the experimental verification of our method. C-scan is the main working mode of the SAM system. Here is how the C-scan works: For a material, any change to the interior uniformity may alter its acoustic impedance. The incident acoustic wave will be partially reflected by the material. The remaining wave will penetrate the sample or interface (e.g. gain boundary, crack, cavity and delamination). These changes are reflected on the amplitude and phase of the echo signals received by the transducer. The structure of a profile in the sample can be displayed in real time, if the waveform data (e.g. peak and time) of each vertical incident point on the sample are shown in different colors or gray values.

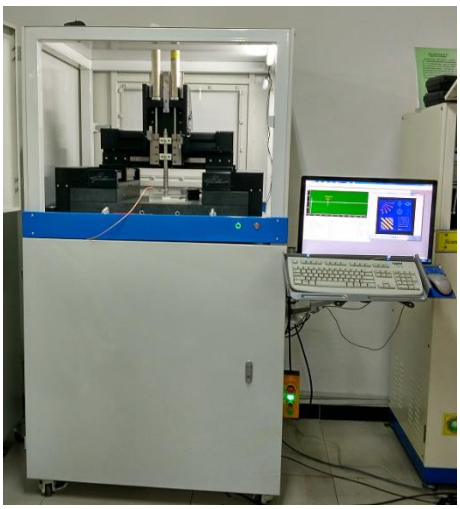

Figure 6. The SAM system

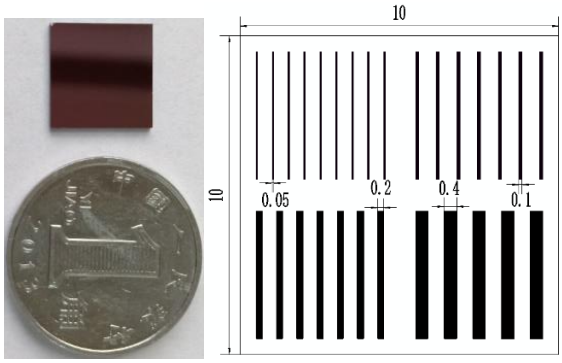

Figure 7. The silicon wafer and the internal structure of the sample

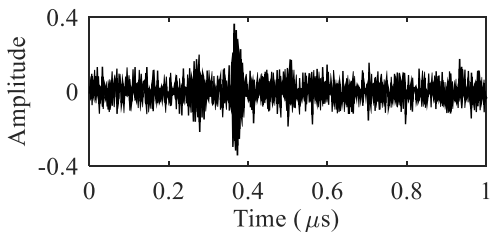

Figure 8. The ultrasonic echo signals from the interfaces inside the sample

The central frequency of the ultrasonic transducer was 100MHz, silicon wafer was selected as the targets, and the sampling frequency was set to 5GHz. The silicon wafer ($10mm \times 10mm \times 0.5mm$) is square on the upper and lower surfaces. Before the experiment, several $150\mu m$-deep grooves with different widths were carved on the silicon wafer by laser etching. Then, the etched silicon wafer was covered with another silicon water of the same size, and the two wafers were bonded into a closed structure. The silicon wafer and the internal structure of the sample are shown in Figure 7.

Figure 8 shows the echo signals from the interfaces inside the sample measured in the experiment. Due to the high testing frequency, the noise in the echo signals was magnified under the high transmission gain. The received signals had a low SNR and multiple peaks, making it hard to the peak and amplitude of the echo signals.

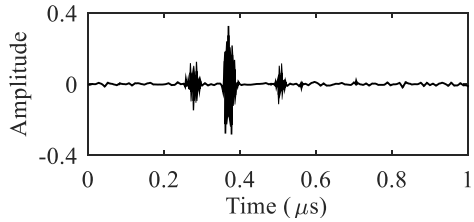

Figure 9. The results of the WST

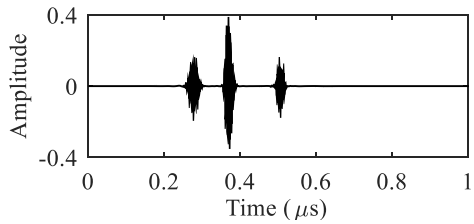

Figure 10. The results of our method

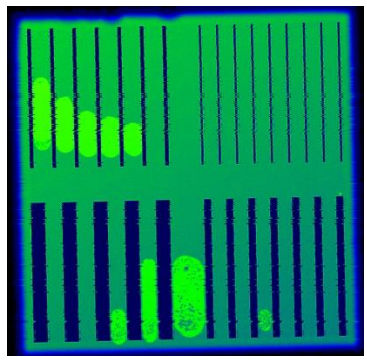

Figure 11. The C-scan image without our method

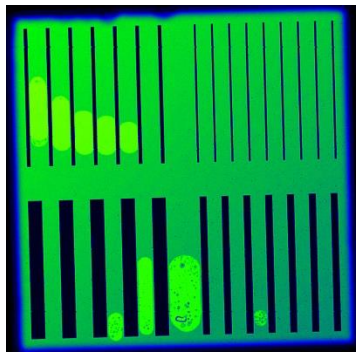

Figure 12. The C-scan image with our method

The denoising results of the WST (Figure 9) indicate severe distortion of the denoised signals. The denoising results of our method are presented in Figure 10. In this figure, the peaks of denoised signals were clear, and the time and amplitude of the signals could be extracted accurately. The comparison verifies the effectiveness of our method.

The SAM system was adopted to perform C-scans of the internal structure of the sample, with or without our method. Without our method, the echo signals from the internal interfaces of the sample were noisy, leading to blurred edges of the internal structure in the C-scan image (Figure 11). With our method, the noise in the echo signals was eliminated, and the internal structure and edges were clear in the C-scan image (Figure 12). The C-scan image obtained by our method facilitates the analysis on the interfaces and internal structure of silicon.

5. CONCLUSIONS

To remove the noise in the echo signals of ultrasonic pulse-echo testing, this paper puts forward a denoising algorithm based on the GST and SVD, which can eliminate the noise in both time- and frequency- domains. The 2D time-frequency matrix, obtained through the GST of ultrasonic echo signals, was subjected to the SVD. Among the SVD results, the large singular values represent useful signals, while small ones represent noise. Then, the threshold for singular values to be zeroed is determined by the ratio between singular entropy increments. During the experiment, the ultrasonic echo signals only contained the first two singular values, which greatly simplifies the denoising process. Our method was applied to denoise simulated ultrasonic echo signals, and the echo signals from the interfaces within a silicon sample. Both simulation and experimental results show that the signals denoised by our method had high SNRs, and that our method achieved better denoising effect than the WST when the original signals have a low SNR. Finally, the SAM system was adopted to perform C-scans of the internal structure of the sample, with or without our method. The results indicate that the C-scan image with our method was much better than that without our method.

The future research will tackle the following issues: (1) The effects of time- and frequency-domain factors *a* and *b* in the window function of the GST on the denoising results; (2) The denoising performance of our method on echo signals from complex interfaces (e.g. nonuniform coating) and the echo signals after multiple superpositions.

REFERENCES

[1] Apostoloudia, A., Douka, E., Hadjileontiadis, L.J., Rekanos, I.T., Trochidis, A. (2007). Time–frequency analysis of transient dispersive waves: A comparative study. Applied Acoustics, 68(3): 296-309. https://doi.org/10.1016/j.apacoust.2006.02.002

[2] Jian, X., Guo, N., Dixon, S. (2005). Ultrasonic weak bond evaluation in ic packaging. Measurement Science and Technology, 17(10): 2637-2642. https://doi.org/10.1088/0957-0233/17/10/015

[3] Siqueira, M.H.S., Gatts, C.E.N., Da Silva, R.R. (2004). The use of ultrasonic guided waves and wavelets analysis in pipe inspection. Ultrsonics, 41(10): 785-797. https://doi.org/10.1016/j.ultras.2004.02.013

[4] Lee, U., Kim, S. (2006). Identification of multiple directional damages in a thin cylindrical shell. International Journal of Solids and Structures, 43(9): 2723-2743. https://doi.org/10.1016/j.ijsolstr.2005.03.077

[5] Keji, Y. (2005). An adaptive filter based on artificial neural net and its application in ultrasonic testing. Chinese Journal of Scientific Instrument, 26(8): 813-817. https://doi.org/10.3321/j.issn:0254-3087.2005.08.011

[6] Song, W., Wang, X., Li, M. (2007). Study on the denoising method for the electromagnetic ultrasonic echoes from multiple interfaces. Acta Acustica, 32(3): 226-231. https://doi.org/10.3321/j.issn:0371-0025.2007.03.005

[7] Kopsinis, Y., Mclaughlin, S. (2009). Development of EMD-based denoising methods inspired by wavelet thresholding. IEEE Transactions on Signal Processing, 57(4): 1351-1362. https://doi.org/10.1109/tsp.2009.2013885

[8] Haddad, S., Bouhadjera, A., Grimes, M., Benkedidah, T. (2011). A New ultrasonic signal processing scheme for detecting echoes of different spectral characteristics in concrete using empirical mode decomposition. Russian Journal of Nondestructive Testing, 47(9): 642-649. https://doi.org/10.1134/S106183091109004X

[9] Sharma, G.K., Kumar, A., Jayakumar, T. (2015). Ensemble empirical mode decomposition-based methodology for ultrasonic testing of coarse grain austenitic stainless steels. Ultrasonics, 57: 167-178. https://doi.org/10.1016/j.ultras.2014.11.008

[10] Gan, J., Zhang, Y. (2003). A study of singular value decomposition of face image matrix. Neural Networks and Signal Proeessing, 1: 197-199. https://doi.org/10.1109/ICNNSP.2003.1279245

[11] Cai, H., Xu, C., Zhou, S. (2015). Study on the thick-walled pipe ultrasonic signal enhancement of modified S-transform and singular value decomposition. Mathematical Problems in Engineering, 52(3): 351-363. https://doi.org/10.1155/2015/312620

[12] Li, Y., Wang, H., Chen, J. (2007). Research of noise reduction of underwater acoustic signals based on singular spectrum analysis. Systems Engineering and Electronics, 29(4): 524-527. https://doi.org/10.3321/j.issn:1001-506X.2007.04.006

[13] Liu, J.G., Li, Z.S., Liu, D. (2006). Features of underwater echo extraction based on SWT and SVD. Acta Acustica, 31(2): 167-172. https://doi.org/10.3321/j.issn:0371-0025.2006.02.012

[14] Zeng, X., Zhou, X., Yang, C. (2016). Ultrasonic defect echoes identification based on empirical mode decomposition and S-transform. Transactions of the Chinese Society for Agricultural Machinery, 47(11): 414-420. https://doi.org/10.6041/j.issn.1000-1298.2016.11.056

[15] Mansinha, L., Stockwell, R.G., Lowe, R.P. (1997). Pattern analysis with two-dimensional spectral localisation: Applications of two-dimensional S transforms. Physica A, 239(1-3): 286-295. https://doi.org/10.1016/s0378-4371(96)00487-6

[16] McFadden, P.D., Cook, J.G., Forster, L.M. (1999). Decomposition of gear vibration signals by the generalised S transform. Mechanical Systems and Signal Processing, 13(5): 691-707. https://doi.org/10.1006/mssp.1999.1233

[17] Pinnegar, C.R., Mansinha, L. (2003). The S-transform with windows of arbitrary and varying shape. Geophysics, 68(1): 381-385. https://doi.org/10.1190/1.1543223

[18] Schimmel, M., Gallart, J. (2005). The inverse S-transform in filters with time-frequency localization. Ieee Transactions on Signal Processing, 53(11): 4417-4422. https://doi.org/10.1109/tsp.2005.857065

[19] Stockwell, R.G., Mansinha, L., Lowe, R.P. (1996). Localization of the complex spectrum: The S transform. Ieee Transactions on Signal Processing, 44(4): 998-1001. https://doi.org/10.1109/78.492555

[20] Shannon, C.E. (1948). A mathematical theory of communication. Bell Labs Technical Journal, 1948(27): 379-433. https://doi.org/10.1002/j.1538-7305.1948.tb00917.x